Photochemical Formation of Ferrimagnetic Chains from a Pair of Polymeric Complexes Made of Octahedral Bis(hexafluoroacetylacetonato)manganese(II) with Diazodi(4-pyridyl)methane in the Cis and Trans Configurations as Repeating Units

Satoru Karasawa, Yoko Sano, Takeyuki Akita, Noboru Koga,* Tetsuji Itoh,† Hiizu Iwamura,† Pierre Rabu,‡ and Marc Drillon‡

Contribution from the Faculty of Pharmaceutical Sciences, Kyushu University, Fukuoka 812-8582, Japan, Institute for Fundamental Research in Organic Chemistry, Kyushu University, Fukuoka 812-8581, Japan, and Institut de Physique et Chemie des Matériaux de Strasbourg, Unité Mixte CNRS-ULP-EHICS (UMR 046), 23, rue due Loess, F-67037 Strasbourg Cedex, France

Received April 16, 1998

Abstract: Two kinds of 1:1 manganese complexes **a** and **b** of bis(hexafluoroacetylacetonato)manganese(II) coordinated with diazodi(4-pyridyl)methane (**1**) were prepared. Complexes **a** and **b** crystallize in the orthorhombic space group *Pbca* and in monoclinic *C*2/*c*, respectively. Two pyridyl nitrogen atoms from two different molecules of **1** are coordinated in the cis and trans configurations to the manganese ion to form helical and zigzag infinite chains of octahedral manganese complexes in complexes **a** and **b**, respectively. The magnetic susceptibilities (χ_{mol}) of both crystals before and after irradiation were measured on a SQUID susceptometer and revealed $\chi_{mol}T$ vs T plots characteristic of *ferrimagnetic chains* after irradiation for 97 h; interaction between the manganese(II) ion and the photogenerated carbene is antiferromagnetic in both complexes. The antiferromagnetic exchange coupling parameters (J) in the photolyzate of complex **a** and **b** were estimated by a theoretical treatment through a procedure of extrapolation by using small rings to be $J/k_B = -34.8 \pm 0.8$ and -24.4 ± 0.5 K, respectively. Maximum $\chi_{mol}T$ values of 210 at 5 K for cis- and 246 emu·K·mol^{-1} at 1.9 K for trans complexes correspond to correlation lengths of 186 and 218 manganese−carbene $S = {}^3/_2$ units, respectively.

Introduction

Hetero-spin systems formed by self-assembly of organic free radicals and metal ions[1] appear to be one of the most promising design strategies for usable molecular-based magnets.[2] Successful examples are two- and three-dimensional ferri/ferromagnets having bis- and tris(*tert*-butylaminoxyl radicals) coordinated to bis(hexafluoroacetylacetonato)manganese(II), Mn(hfac)$_2$.[3] In these spin systems, organic radicals served not only as spin carriers but also as ligating sites to magnetic metal ions. Alternatively, we have taken into consideration pyridine and imidazole bases carrying organic free radicals as ring substituents. Systematic studies revealed that the sign and the magnitude of the exchange coupling between 2p spins of the radical centers and the metal 3d spins are controlled by the regiochemistry of the radical center on the pyridine ring in 1:2 manganese(II) or copper(II) complexes with 3- and 4-pyridyl(*N*-*tert*-butyl)aminoxyls, [Mn(hfac)$_2$(3- and 4NOPy)$_2$] or [Cu(hfac)$_2$(3- and 4NOPy)$_2$], in good agreement with the spin

* Address correspondence to this author at the Faculty of Pharmaceutical Sciences, Kyushu University.

† Institute for Fundamental Research in Organic Chemistry, Kyushu University.

‡ Unité Mixte CNRS-ULP-ERHICS.

(1) (a) Eaton, G. R.; Eaton, S. S. *Acc. Chem. Res*. **1988**, *21*, 107. (b) Caneschi, A.; Gatteschi, D.; Laugier, J.; Rey, P.; Sessoli, R. *Inorg. Chem*. **1988**, *27*, 1553. (c) Caneschi, A.; Gatteschi, D.; Renard, J. P.; Rey, P.; Sessoli, R. *Inorg. Chem*. **1989**, *28*, 1976. (d) Caneschi, A.; Gatteschi, D.; Sessoli, R.; Rey, P. *Acc. Chem. Res*. **1989**, *22*, 392. (e) Caneschi, A.; Gatteschi, D.; Rey, P.; Sessoli, R. *Inorg. Chem*. **1991**, *30*, 3936. (f) Burdukov, A. B.; Ovcharenko, V. I.; Ikorski, V. N.; Pervukhina, N. V.; Podberezskaya, N. V.; Grigor'ev, I. A.; Larionov, S. V.; Volodarsky, L. B. *Inorg. Chem*. **1991**, *30*, 972. (g) Caneschi, A.; Dei, A.; Gatteschi, D. *J. Chem. Soc., Chem. Commun*. **1992**, 630. (h) Caneschi, A.; Chiesi, P.; David, L.; Ferraro, F.; Gatteschi, D.; Sessoli, R. *Inorg. Chem*. **1993**, *32*, 1445. (i) Stumpf, H. O.; Ouahab, L.; Pei, Y.; Grandjean, D.; Kahn, O. *Science* **1993**, *261*, 447. (j) Volodarsky, L. B.; Reznikov, V. A.; Ovcharenko, V. I. *Synthetic Chemistry of Stable Nitroxides*, CRC Press: Boca Raton, FL, 1994; Chapter 4.

(2) (a) Kahn, O. *Molecular Magnetism*; VCH Publishers: Weinheim, 1993. (b) Gatteschi D. *Adv. Mater*. **1994**, *6*, 635. (c) Miller, J. S.; Epstein, A. J. *Angew. Chem., Int. Ed. Engl*. **1994**, *33*, 385. (d) Miller, J. S.; Epstein, A. J. *Chem. Eng. News* **1995**, *October 2*, 30. (e) Kahn, O., Ed. *Magnetism: A Supramolecular Function*; NATO ASI Series C, Kluwer: Dordrecht, 1996. (f) Turnbull, M. M.; Sugimoto, T.; Thompson, L. K., Eds. *Molecule-based magnetic materials*; ACS Symp. Ser. 644; American Chemical Society: Washington, DC, 1996. (g) Gatteschi, D. *Curr. Opin. Solid State Mater. Sci*. **1996**, *1*, 192.

(3) (a) Inoue, K.; Iwamura, H. *J. Am. Chem. Soc*. **1994**, *116*, 3173. (b) Inoue, K.; Iwamura, H. *J. Chem. Soc., Chem. Commun*. **1994**, 2273. (c) Inoue, K.; Iwamura, H. *Synth. Met*. **1995**, *71*, 1791. (d) Inoue, K.; Hayamizu, T.; Iwamura, H. *Mol. Cryst. Liq. Cryst*. **1995**, *273*, 67. (e) Inoue, K.; Hayamizu, T.; Iwamura, H. *Chem. Lett*. **1995**, 745. (f) Mitsumori, T.; Inoue, K.; Koga, N.; Iwamura, H. *J. Am. Chem. Soc*. **1995**, *117*, 2467. (g)Inoue, K.; Hayamizu, T.; Iwamura, H.; Hashizume, D.; Ohashi, Y. *J. Am. Chem. Soc*. **1996**, *118*, 1803. (h) Inoue, K.; Iwamura, H. *Adv. Mater*. **1996**, *8*, 73. (i) Oniciu, D. C.; Matsuda, K.; Iwamura, H. *J. Chem. Soc., Perkin Trans. 2* **1996**, 907. (j) Iwamura, H.; Inoue, K.; Hayamizu, T. *Pure Appl. Chem*. **1996**, *68*, 243. (k) Inoue, K.; Iwamura, H. *Mater. Res. Soc. Symp. Proc*. **1996**, *413*, 313.

S0002-7863(98)01293-1 CCC: $15.00
Published on Web 09/16/1998

polarization mechanism of the π-electrons on the pyridine ring.[4] Furthermore, the sign of the exchange coupling was found to depend also on whether the spin-containing 2p-orbital at the nitrogen overlaps with the singly occupied 3d orbital at the metal ions as in the d_{xz} orbital of Mn(II) or is orthogonal to it as in $d_{x^2-y^2}$ orbital of Cu(II).[4a,b]

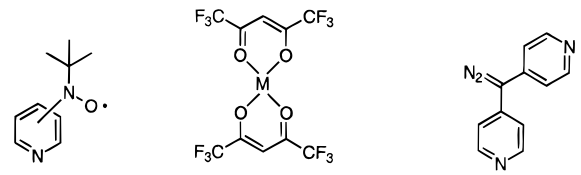

On the basis of the knowledge from the 1:2 model complexes, diazodi(4-pyridyl)methane (**1**) having a diazo group, a precursor to a triplet carbene, was designed as a bridging ligand. By employing carbenes generated from photolysis of the diazo moieties, it is possible to add the function of photoresponse to the ligand, which already serves as an organic spin source and a magnetic coupler. Polymeric 1:1 complexes of $M(hfac)_2$ (M = Cu(II) and Mn(II)) with **1** were prepared.[5,6] In a previous paper we reported the crystal structure of [$Cu(hfac)_2$·**1**] and the formation of *ferromagnetic chains* after its irradiation. However, interchain antiferromagnetic interaction dominated the low-temperature magnetic properties and the correlation length along the ferromagnetic chains was estimated to be only ca. 23 units at 3 K.[5a] In the corresponding manganese complexes with **1**, cis and trans complexes, [$Mn(hfac)_2$·**1**]s, were obtained separately for which we have been able to obtain X-ray molecular and crystal structures, and much extended correlation lengths after photolysis.[6]

Experimental Section

General Methods. Infrared spectra were measured on a Hitachi 270-30 IR spectrometer. Thermal analyses were performed on a Riken DSC 8240 differential scanning calorimeter. Melting points were obtained with a MEL-TEMP heating block and are uncorrected. Elemental analyses were performed in the Analytical Center of Faculty of Science in Kyushu University.

X-ray Crystal and Molecular Structural Analyses. All diffraction data were collected on a Rigaku RAXIS-IV imaging plate area detector system attached with a liquid-nitrogen cooling system. The incident radiation consisted of Mo Kα X-rays generated by a rotating anode X-ray generator fitted with a graphite monochromator and operated at 45 kV and 300 mA. The oscillation angle used for complexes **a** and **b** was 5° and each data frame was exposed for 30 and 45 min, respectively. Totals of 18 and 20 data frames for **a** and **b**, respectively, were collected and processed with the RAXIS control software. Pertinent crystallographic parameters and refinement data are collected in Table 1.

The structures of complexes **a** and **b** [$Mn(hfac)_2$·**1**] were solved in *Pbca*(No. 61) and *C*2/*c*(No. 15), respectively, by direct methods[7] and refinement converged by using the full-matrix least squares of the teXsan[8] crystallographic software package (Version 1.8). All non-hydrogen atoms were refined anisotropically; hydrogen atoms were included at standard positions (C−H 0.96 Å, C−C−H 120°) and refined isotropically with use of a rigid model.

Table 1. Crystallographic Data and Experimental Parameters

	complex **a**	complex **b**
empirical formula	$C_{21}H_{10}N_4O_4F_{12}Mn$	$C_{21}H_{10}N_4O_4F_{12}Mn$·$2C_7H_8$
formula wt	665.25	849.53
cryst color, habit	red, cubic	orange, plate
cryst dimens (mm)	0.2 × 0.2 × 0.2	0.2 × 0.2 × 0.1
cryst system	orthorhombic	monoclinic
lattice params		
a (Å)	21.792(2)	13.69(2)
b (Å)	18.511(5)	13.669(3)
c (Å)	13.358(4)	20.864(5)
β (deg)		96.184(4)
V (Å^3)	5388(3)	3881(3)
space group	*Pbca* (No. 61)	*C2/c* (No. 15)
Z value	8	4
D_{calc} (g/cm^3)	1.640	1.454
no. of observations	2276	1822
no. of variables	380	277
residual: *R*; *Rw*	0.062; 0.061	0.065; 0.079

Magnetic Measurements. Magnetic susceptibilities were measured on Quantum Design $MPMS_2$ (0−10 kOe) and MPMS (0−50 kOe) SQUID magnetometer/susceptometers. Data were corrected for the magnetization of a sample holder, a quartz cell, and the lid used and for diamagnetic contributions which were estimated from Pascal's constants.

Magnetic measurements of ca. 0.5 mg fine crystalline samples were performed before and after irradiation with light (λ = 514 nm) from an argon ion laser through an optical fiber inserted into the SQUID magnetometer/susceptometer at about 5 K. The light intensity at the inside edge of the optical fiber was determined prior to the experiment by using a laser power meter to be ca. 35 mW. The degree of the photolysis was estimated by comparing the absorptivity at 2067 cm^{-1} for [$Mn(hfac)_2$·**1**] due to the diazo groups of the complexes before and after the photolysis. The progress of the photolysis was found not to be even. Formation of the carbene species on the irradiated side of the crystals is judged to be higher than the average figures. Temperature dependencies of the molar magnetic susceptibility χ_{mol} (gram susceptibility times the formula weight of the complexes) for [$Mn(hfac)_2$·**1**] in the range 1.9−300 K were measured at constant fields of 20, 100, 500, and 5000 Oe in the temperature range of 1.9−6.0, 6.5−14, 16−30, and >32 K, respectively.

Materials. Dichloromethane was distilled under high-purity Ar after drying with calcium hydride. All reactions were stirred under an atmosphere of Ar. $Mn(hfac)_2$·$2H_2O$ was prepared by the standard procedure. Diazodi(4-pyridyl)methane (**1**) was prepared by a procedure reported previously.[5]

Complex a of [$Mn(hfac)_2$·1]. For the preparation of a solution of nonaqua $Mn(hfac)_2$, a solution of 0.27 g of [$Mn(hfac)_2$·$2H_2O$] in 50 mL of *n*-heptane was heated and reduced to 30 mL by distillation. The solution was cooled under a dry nitrogen atmosphere. To a still warm *n*-heptane solution was added a solution of 0.1 g of **1** in 30 mL of CH_2Cl_2. The resulting orange powder was collected. Complex **a** was obtained as red cubes by recrystallization from MeOH: IR (KBr) 2068 cm^{-1}. Anal. Calcd for $C_{21}H_{10}N_4O_4F_{12}Mn$: C, 37.92; H, 1.52; N, 8.42. Found: C, 37.82; H, 1.59; N, 8.49.

Complex b of [$Mn(hfac)_2$·1]. Solutions of **1** in CH_2Cl_2 and [$Mn(hfac)_2$·$2H_2O$] in CH_2Cl_2−MeOH were mixed in a 1:1 molar ratio

(4) (a) Ishimaru, Y.; Kitano, M.; Kumada, H.; Koga, N.; Iwamura, H. *Inorg. Chem.* **1998**, *37*, 2273. (b) Kitano, M.; Ishimaru, Y.; Inoue, K.; Koga, N.; Iwamura, H. *Inorg. Chem.* **1994**, *33*, 6012. (c) Kitano, M.; Koga, N.; Iwamura, H. *J. Chem. Soc., Chem. Commun.* **1994**, 447. (d) Ishimaru, Y.; Inoue, K.; Koga, N.; Iwamura, H. *Chem. Lett.* **1994**, 1693.

(5) (a) Sano, Y.; Tanaka, M.; Koga, N.; Matsuda, K.; Iwamura, H.; Rabu, P.; Drillon, M. *J. Am. Chem. Soc.* **1997**, *119*, 8246. (b) Koga, N.; Iwamura, H. *Mol. Cryst. Liq. Cryst.* **1997**, *305*, 415. (c) Karasawa, S.; Tanaka, M.; Koga, N.; Iwamura, H. *J. Chem. Soc., Chem. Commun.* **1997**, 1359.

(6) Preliminary accounts of this work have appeared in: Koga, N.; Ishimaru, Y.; Iwamura, H. *Angew. Chem., Int. Ed. Engl.* **1996**, *35*, 755 and ref 5b.

(7) MULTAN88 for complex **a**: Debaerdemaaeker, T.; Germain, G.; Main, P.; Refaat, L. S.; Tate, C.; Woolfson, M. M. **1988**. Computer programs for the automatic solution of crystal structures form X-ray diffraction data, University of York, U.K. SHELXS86 for complex **b**: Sheldrick, G. M. Crystallographic Computing 3; Sheldrick, G. M., Kruger, C., Goddard, R., Eds.; Oxford University Press: New York, 1985. pp 175−189.

(8) Crystal Structure Analysis Package, Molecular Structure Corporation (1985 and 1992).

Table 2. Selected Bond Lengths, Bond Angles, and Dihedral Angles for Complexes **a** and **b**

	complex **a**		complex **b**	
bond lengths (Å)	Mn−O1	2.167(6)	Mn−O1	2.168(5)
	Mn−O2	2.155(5)	Mn−O2	2.163(5)
	Mn−O3	2.178(6)	Mn−N1	2.233(5)
	Mn−O4	2.161(5)		
	Mn−N1	2.240(7)		
	Mn−N2	2.247(7)		
bond angles (deg)	N1−Mn−N2	86.5(2)	N1−Mn−N1*	180.0
	N1−Mn−O3	171.5(3)	N1−Mn−O3	177.9
	N2−Mn−O1	172.2(3)	C3−C6−C3*	126.8
	O2−Mn−O4	177.0(2)		
	Mn−N1−C3	176.2		
	Mn−N2−C9	175.5		
	C3−C6−C9	127.0(6)		
dihedral angle (deg)	C1C3C5−C7C9C11	59.0[a]	C1C3C5−C1*C3*C5*	49.3[a]
	N1C2C4−N2C8C10	79.6[b]	N1C2C4−N1*C2*C4*	0[b]

[a] Through the diazo moiety. [b] Through the manganese.

at room temperature. The resulting orange powder was collected. Complex **b** was obtained as orange plates by recrystallization from MeOH−toluene: IR (KBr) 2067 cm^{-1}. Anal. Calcd for $C_{21}H_{10}N_4O_4F_{12}Mn \cdot 0.6C_7H_8$: C, 42.01; H, 2.07; N, 7.78. Found: C, 41.77; H, 2.13; N, 7.89.

Results

Preparations of Manganese Complexes Coordinated with 1. Isomeric 1:1 manganese complexes **a** and **b** of [Mn(hfac)$_2$·**1**] could be obtained individually as red cubes and orange plates by using Mn(hfac)$_2$ and Mn(hfac)$_2$·2H$_2$O with **1**, respectively. The elemental analysis of the latter complex suggested that the crystalline sample contained toluene molecules employed for the recrystallization.

In differential scanning calorimetry (20 °C/h) for both complexes, exothermic peaks were observed at 102 °C for complex **a** and 96 and 110 °C for **b**; free ligand **1** showed an exothermic peak at 133 °C under similar conditions.

Molecular and Crystal Structures of Complexes a and b of [Mn(hfac)$_2$·1]. Both samples were too fragile to stand ambient temperature measurements. Molecular and crystal structures of both complexes **a** and **b** have been solved by X-ray analysis with use of an imaging plate at −100 and −80 °C, respectively. Crystallographic data and experimental parameters for complexes **a** and **b** are summarized in Table 1. Selected bond lengths, bond angles, and dihedral angles are given in Table 2.

As shown in the ORTEP drawings of Figures 1a and 2a, two complexes **a** and **b** make a significant difference in the molecular structures. Two pyridyl nitrogen atoms in complexes **a** and **b** are coordinated to the manganese(II) ion in the cis and trans configuration, respectively. The geometries around manganese ions for both complexes were illustrated in Figure 3. The molecular structure of complex **a** has no molecular symmetry and consists of a series of distorted octahedra as seen in bond angles and bond lengths around the manganese(II) ion as listed in Table 2. The pyridine planes coordinated to the Mn(II) are facing O(3) or O(1) of hfac and each other; the dihedral angles of O(2)MnN(1)−N(1)C(2)C(4) and O(2)MnN(2)−N(2)C(8)C(10) and the torsion angles N(1)MnN(2)C(7) and N(2)MnN(1)C(1) are 3.87, 4.18, 82.4, and 87.5°, respectively. On the other hand, the manganese(II) ion of complex **b** resides in the center of symmetry of an elongated octahedron in which bond lengths are Mn−O(1) = 2.168(5) Å, Mn−O(2) = 2.163(5) Å, and Mn−N(1) = 2.233(5) Å (Table 2). The planes of the coordinated pyridine ligands are directed to the methine carbons of hfac groups; the dihedral angle of O(2)MnN(1)−N(1)C(2)C(4) is 41.03° and tilted slightly (by 2.7°) toward methine carbon C(9). In this crystal of complex **b**, C(7)F$_3$ groups and two toluene molecules of crystallization were observed to be disordered.

Bond angles C(3)−C(6)−C(9) for complex **a** and C(3)−C(6)−C(3*) for **b** are 127.0(6) and 126.8°, respectively. The dihedral angles between the pyridine rings around diazo moiety are 59.01 and 49.25° for complexes **a** and **b**, respectively. Compared with those for free ligand **1**, the former and the latter angles become slightly smaller and larger, respectively, by the complexation with manganese ion (corresponding angles for **1** are 128.5 and 42.4°, respectively).[5]

Crystal structures of complexes **a** and **b** showed a notable difference caused by cis and trans coordination of the pyridine units. Manganese ions aligned alternately at two positions on *b* axis for complex **a** and linearly at one point for complex **b**. Two pyridine groups of **1** connect these manganese ions to form a polymeric chain. As shown in Figures 1b and 2b, complexes **a** and **b** have a helical structure (see projection from the *c* axis in Figure 1c) in which four chains around a given chain show opposite helicity and a zigzag structure, respectively. The manganese ions are 11.81 (Mn(1)−Mn(2)) and 6.70 Å (Mn(1)−Mn(2*)) apart along the chains for complex **a** (Figure 1b) and 11.84 Å for **b**, suggesting that the manganese ions are considered to be magnetically isolated. The helical chains in complex **a** run along the *c* axis and have two kinds of two sets of neighboring chains in the directions of the *a* and *b* axes with distances of 3.06 {between the terminal nitrogen atoms of the diazo moieties (N(4)−N(4*))} and 4.43 Å {between the carbons of pyridine rings (C(11) −C(5*))}, respectively, in which the latter atoms belong to the nearest chain (Figure 1b). Taking liberation of dinitrogen molecules after photolysis and the relative geometry of the pyridine rings between the chains into account, the observed short distances might be insignificant for magnetic properties of photoproducts for complex **a**. No short contacts within 4 Å between the chains of complex **b** were observed (Figure 2c). The chains in complex **b** are regarded to be well separated (>7 Å) by toluene molecules of crystallization.

Magnetic Measurements of Complexes a and b. (A) Development of *M* Values after Irradiation. Photolysis of the solid samples placed in a sample cell was carried out at 5−8 K with light (λ = 514 nm) from an argon ion laser through an optical fiber. The development of *M* values at 5 and 2 K at a constant field of 100 Oe for complexes **a** and **b** after irradiation is shown in Figure 4. *M* values after irradiation within 15 and 10 min surpassed theoretical values, 108 and 268 emu·Oe·mol^{-1}

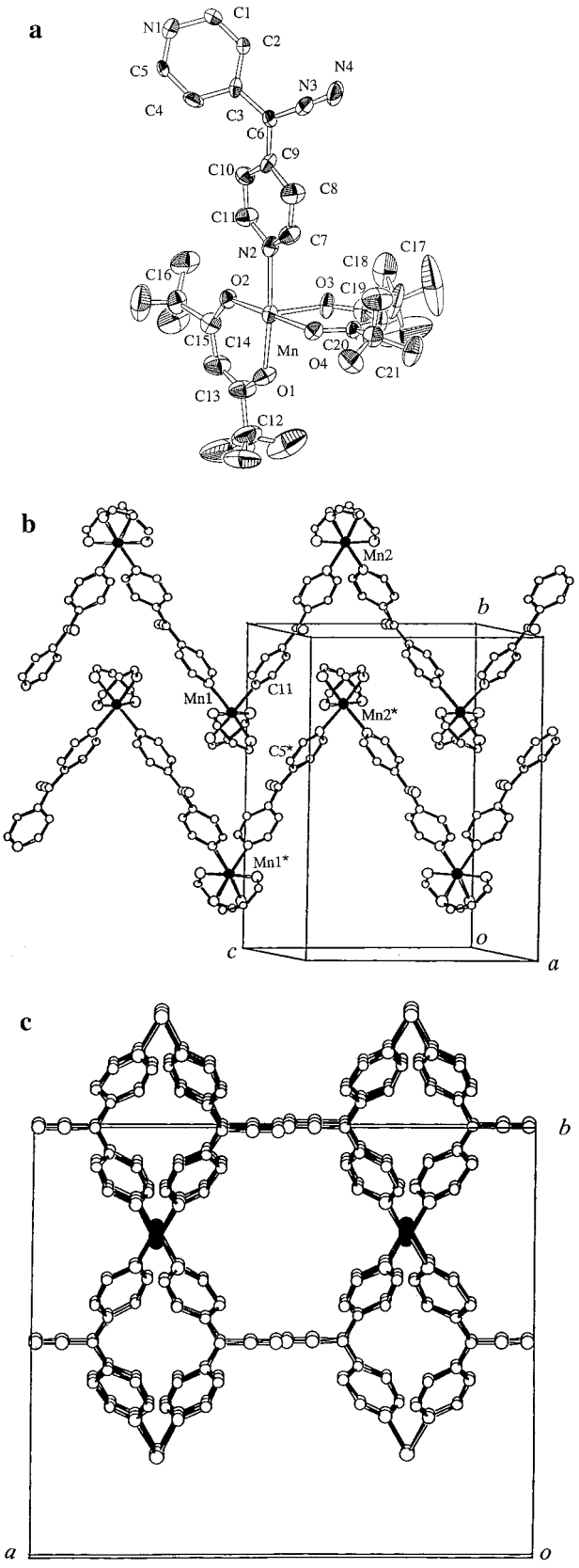

Figure 1. (a) ORTEP drawing of the molecular structure for one unit of complex **a** of [Mn(hfac)$_2$·**1**], using 50% probability ellipsoids. (b) Ball-and-stick model of the crystal structure for complex **a** and (c) the one projecting from the *c* axis. The trifluoromethyl groups have been omitted for the sake of clarity.

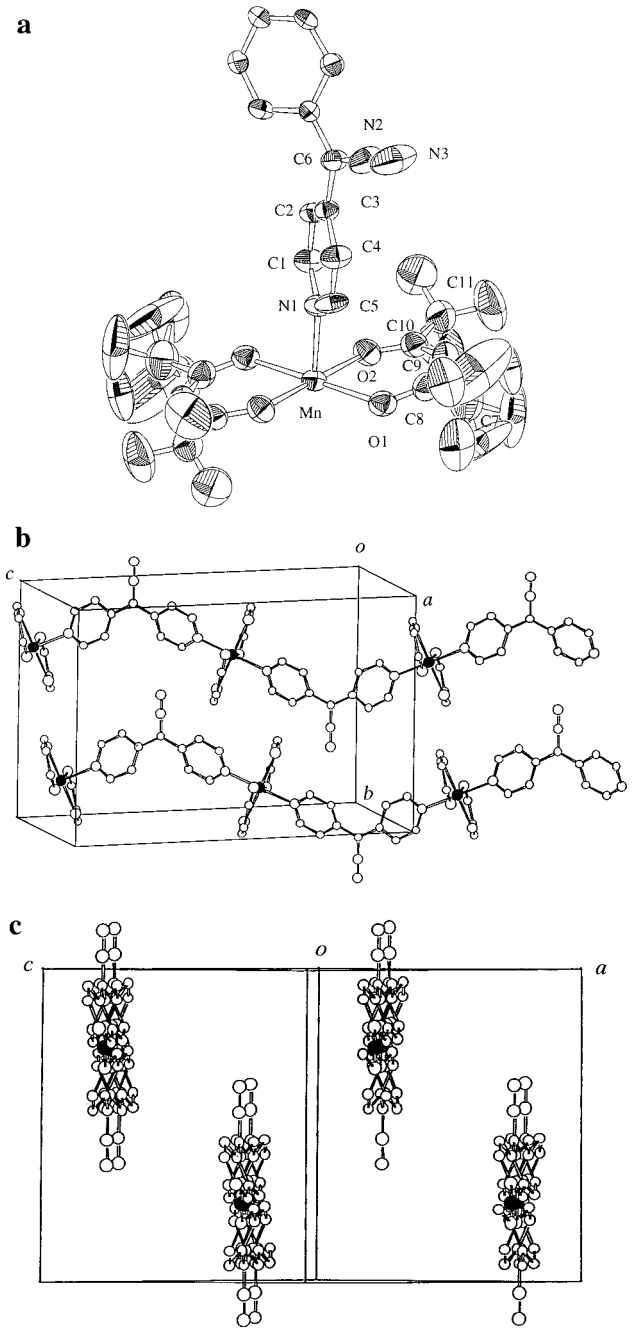

Figure 2. (a) ORTEP drawing of the molecular structure for one unit of complex **b** of [Mn(hfac)$_2$·**1**], using 50% probability ellipsoids. (b) Ball-and-stick model of the crystal structure for complex **b** and (c) the one projecting from the *ac* diagonal axis. The trifluoromethyl groups and toluene molecules have been omitted for the sake of clarity.

at 5 and 2 K, respectively, calculated for a sum of 100% generation of the $S = 2/2$ carbene and the isolated $S = 5/2$ manganese ion. Even after irradiation for 97 h, M values increased slowly. The intensities of IR absorptions at 2068 and 2067 cm^{-1} due to diazo moieties for complexes **a** and **b** were found after the magnetic measurement on a SQUID to have decreased to 11 and 28% of the original values, respectively.

(B) Temperature Dependence of Magnetic Susceptibility. The observed molar paramagnetic susceptibility (χ_{mol}) data were expressed in the form of $\chi_{mol}T$, which is more closely related to effective magnetic moment by $\mu_{eff} = (3\chi_{mol}kT/N)^{1/2}$. Before irradiation, $\chi_{mol}T$ values of fine crystalline samples of both isomers were nearly constant at 2−300 K and values of 3.52 and 3.69 emu·K·mol^{-1} at 300 K were close to a theoretical

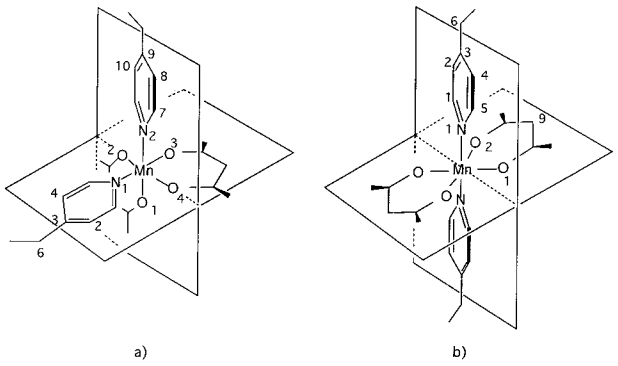

Figure 3. Schematic drawings around manganese ions in (a) complex **a** and (b) complex **b**.

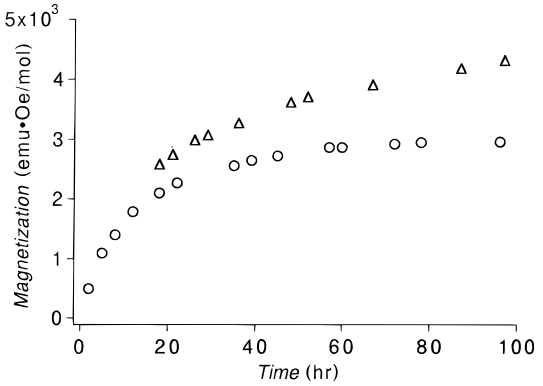

Figure 4. Developments of the *M* values in 100 Oe for complex **a** (○) at 5 K and **b** (△) at 2 K with irradiation time

spin-only value of 4.37 emu·K·mol^{-1} expected for paramagnetic samples of $S = 5/2$.[9,10]

The $\chi_{mol}T$ values for both samples changed with irradiation time and the gradual changes continued even after 97 h (Figures 5 and 6). At high temperature, $\chi_{mol}T$ values were lower than 5.37 emu·K·mol^{-1} expected for one $S = 5/2$ and one $S = 1$ spins in the paramagnetic state. As the temperature was decreased from 230 K, $\chi_{mol}T$ values for complexes **a** and **b** decreased gradually to a shallow minimum of 3.58 and 3.16 emu·K·mol^{-1} at ca. 80 K, respectively, and rapidly increased. While the $\chi_{mol}T$ values for complex **a** reached a maximum of 210 emu·K·mol^{-1} at 5 K and then decreased until 1.9 K, those for complex **b** did not reach a maximum above 1.9 K (246 emu·K·mol^{-1} at 1.9 K). Abrupt changes in the $\chi_{mol}T$ values were observed at 230 K above which they traced a horizontal line before irradiation. Subsequent measurements of the $\chi_{mol}T$ values at 2−300 K of the same sample left at 300 K for an hour showed temperature-independent horizontal lines overlapped with those before irradiation. Discontinuous changes in $\chi_{mol}T$ values observed at ca. 50 K are most probably due to the adsorbed oxygen.

(C) Field Dependence of Magnetization. For both complexes of [Mn(hfac)$_2$·**1**], not only temperature dependence of χ_{mol} but also field dependence of the magnetization (*M*) were investigated alternately for a given sample. Field dependence of magnetization (*M*) for complex **a** of [Mn(hfac)$_2$·**1**] at 5 K in the range of 0−50 kOe before and after irradiation is shown in Figure 7. As the irradiation proceeded, *M* values increased in the region 0−20 kOe but decreased at 20−50 kOe compared with those before irradiation. The observed increase and

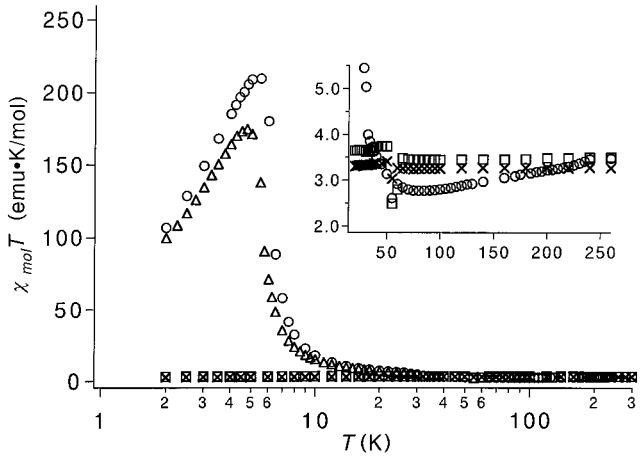

Figure 5. The plots of χ_{mol}·T vs T for a crystalline sample of complex **a**: before (□), after the irradiation for 60 (△) and 97 h (○), and then after being at 300 K for 1 h (×). The "molar" magnetic susceptibility means the one per formula [Mn(hfac)$_2$·**1**] of the crystalline sample. The inset shows the high-temperature region 30−300 K.

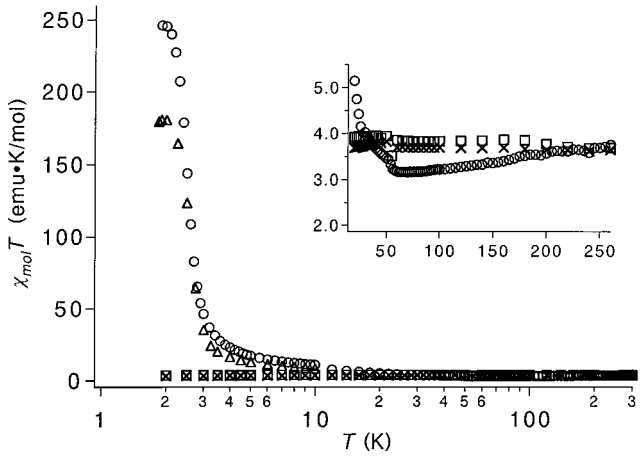

Figure 6. The plots of χ_{mol}·T vs T for a crystalline sample of complex **b**: before (□), after the irradiation for 50 (△) and 97 h (○), and then after being at 300 K for 1 h (×). The "molar" magnetic susceptibility means the one per formula [Mn(hfac)$_2$·**1**] of the crystalline sample. The inset shows the high-temperature region 30−300 K.

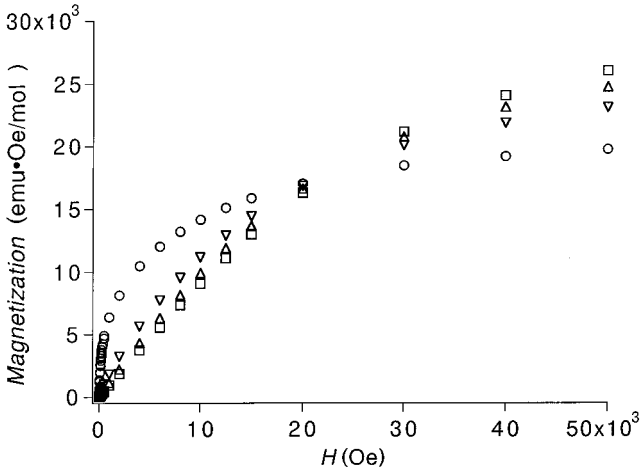

Figure 7. The plot of *M* vs *H* for complex **a**: before (□) and after the irradiation for 1 (△), 4 (▽), and 33 h (○).

(9) The observed discrepancy may be an experimantal error caused by a small change of weight (a possible loss) of the sample during the operation of a degas cycle in SQUID. Improvement of the sample cells for irradiation is in progress.

(10) Since an effective irradiation of microcrystalline samples through a thin optical fiber at cryogenic temperature was required, we could not employ a technique of applying Vaselin or Nujol to prevent the samples from moving within a special sample cell.

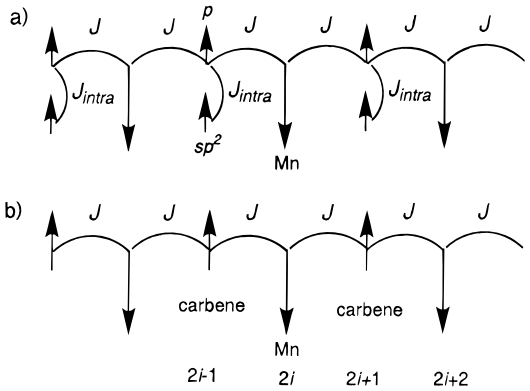

Figure 8. Schematic arrangement of the spins within an alternating chain of [Mn(hfac)$_2$·{di-(4-pyridyl)carbene}]: (a) the Mn−dipycarbene sequence with p−sp^2 spin alignment at the carbene centers; (b) the effective arrangement assuming strong ferromagnetic p−sp^2 coupling.

decrease of M values in the $M-H$ plot clearly indicates the increase of correlation length and the decrease of saturation magnetization caused by antiferromagnetic interaction between the generated carbene and Mn(II).

Furthermore, we came across a puzzling observation that both the field and temperature dependences of the magnetization were dependent on sample history in the magnetic field. These effects, probably due to the orientation of the crystals, were observed in low-temperature region below 10 K.[11]

Theoretical Analysis of the Temperature Dependence of the Magnetic Susceptibility of Complexes a and b After Photolysis. From a magnetochemical point of view, complexes **a** and **b** after photolysis, namely, [Mn(hfac)$_2${di(4-pyridyl)-carbene}], consist of assemblies of alternating chains of $S = 5/2$ (Mn) and pairs of $S = 1/2$ (carbene) spins. The two spins at the carbene centers are localized in the p and the hybridized sp^2 orbitals. Only the former interacts directly with the $S = 5/2$ spin (d^5 orbitals) of the manganese(II) atoms. Further, the two spins at the carbene centers are strongly ferromagnetically coupled to each other due to the one-center orthogonality of the orbitals.[12] Therefore, the spin arrangement may be schematized as in Figure 8, where J and J_{intra} hold for Mn(II)−carbene and intra-carbene spin−spin interactions.

As explained above, a strong ferromagnetic coupling between the two $S = 1/2$ spins at the carbene centers is expected, in agreement with the experimental data. Indeed, the fact that the high-temperature value of the susceptibility is lower than expected indicates that the interactions are strong enough to be efficient at high temperature. At low temperature, the compounds behave as antiferromagnetic chains with uncompensated magnetic moments (ferrimagnetism). Thus, pseudo-spins may be considered. After examination of all the possibilities, the most reliable to the experimental feature is to assume that the intra-carbene-center interaction J_{intra} is strongly ferromagnetic (>300 K), thus stabilizing a triplet ground state for a pair of organic spins. The magnetic chains may thus be described as alternating $S = 5/2$ and 1 antiferromagnetic chains, as illustrated in Figure 8b, where J holds for an effective Mn(II)−carbene exchange interaction. This configuration is fully consistent with the ferrimagnetic experimental behavior. The signs of J and J_{intra} agree with those expected from the literature for manganese−carbene and carbene−carbene exchange couplings.

Assuming that this model is correct, the effective spin Hamiltonian becomes:

$$H = -\sum_i J\,\mathbf{S}_{2i}(\mathbf{S}_{2i-1} + \mathbf{S}_{2i+1}) - \sum_i g\mu_B H\{\mathbf{S}_{2iz} + \mathbf{S}_{(2i+1)z}\} \quad (1)$$

where J refers to the effective exchange interaction between Mn(II) and carbenes, $\mathbf{S}_{2i+1} = 1$ and $\mathbf{S}_{2i} = 5/2$ hold for spin moments of the carbene and the manganese ion, respectively, and g is identical for all sites. The well-known method initiated by Bonner and Fisher for regular chains,[13] using rings of increasing number of basic (Mn−carbene) units, was carried out. Calculations of the magnetic susceptibility[14] were performed for rings of $S = 5/2$ and 1 spin units, as a function of kT/J. An overall g factor of 2.003 was used, which corresponds well to the isotropic character of the spin carriers.

Then, following the method of Drillon et al.,[15] the behavior of the infinite chain was extrapolated from low-temperature values of $\chi T(kT/J)$ obtained for $N = 2$, 4, 6, and 8. The extrapolated curve was fitted as a polynomial function of $x = J/kT$ exhibiting the correct conditions at the limits. The best fits of the extrapolation correspond to the following expression:

$$\chi T = \frac{Ax^3 + Bx^2 + Cx + D}{Ex^2 + Fx + G} \quad (2)$$

with $A = 86.40$, $B = 85.90$, $C = -22.0$, $D/G = 21/4$, $E = 26.56$, and $F = 2.28$.

The experimental data have been fitted by using the above expression for $T > 3$ K. To improve the fits, interchain interaction z_j was introduced by a molecular field:[15]

$$\chi_{corr} = \chi/\{1 - r(z_j/k)\chi\}$$

The best refined values correspond to $J/k_B = -34.8 \pm 0.8$ K, $g = 2.00$, and $z_j = 0.51 \pm 0.02$ K with a scale factor of 0.81 ± 0.01 for complex **a** (Figure 9a). Similarly, $J/k_B = -24.4 \pm 0.5$ K, $g = 2.00$, and $z_j = 0.049 \pm 0.004$ K with a scale factor of 0.88 ± 0.01 for complex **b** (Figure 9b).[16] The minima in the χT vs T plots are well reproduced. The corresponding χT variation is compared with the experimental data in Figure 9.

Discussion

Magnetic Properties of Complexes a and b. Before irradiation, the $\chi_{mol}T$ values not far from 4.37 emu·K·mol^{-1}

(11) Field dependences of M for complexes **a** at 2 K and **b** at 5 K after irradiation for 97 h are shown in Figures S1 and S2, respectively. M values below 500 Oe obtained by increasing the field from 0 to 10 kOe were always lower than those obtained by decreasing the field. However, no remnant magnetization was observed and M disappeared at 0 Oe. In the second measurement of the field dependence of M (see Figure S2), M values appear on the upside and the downside of those for the first run on increasing and decreasing fields, respectively. This strange field dependence of M which was not observed in the $M-H$ plots of [Cu(hfac)$_2$·**1**] obtained under similar conditions, had been obtained from an early stage of photolysis (irradiation time longer than 2 h). No appreciable change of M value was observed after keeping a constant field (<1 kOe) for 120 min, indicating that this phenomena was not due to the slow relaxation of the large magnetic moment. Slight movement of the magnetically anisotropic crystals in the sample cell in the applied field is suggested.[10]

(12) (a) Brandon, R. W.; Closs, G. L.; Davoust, C. E.; Hutchison, C. A., Jr.; Kohler, B. E.; Silbey, R. *J. Chem. Phys.* **1965**, *43*, 2006. (b) Higichi, J. *J. Chem. Phys.* **1963**, *38*, 1237; *39*, 1847. (c) Hutchison, C. A., Jr.; Kohler, B. E. *J. Chem. Phys.* **1969**, 51, 3327.

(13) Bonner, J. C.; Fisher, M. E. *Phys. Rev.* **1964**, *135*, 640.

(14) (a) Reference 2a, pp 26−27. (b) Carlin, R. L. *Magnetochemistry*; Springer-Verlag: Coburg, Germany, pp 132−133.

(15) Coronado, E.; Drillon, M.; Georges, R. In *Research Frontiers in Magnetochemistry*, O'Connor, C. J., Ed.; World Scientific Publishing Co. Ptc. Ltd: Singapore, 1993; p 27.

(16) Calculations for a large number of spins were carried out by using the Cray C98 computer of the French institute for development and means in computer science, IDRIS. A scale factor includes the contribution from the unphotolyzed part of complexes, isolated manganese ions, etc.

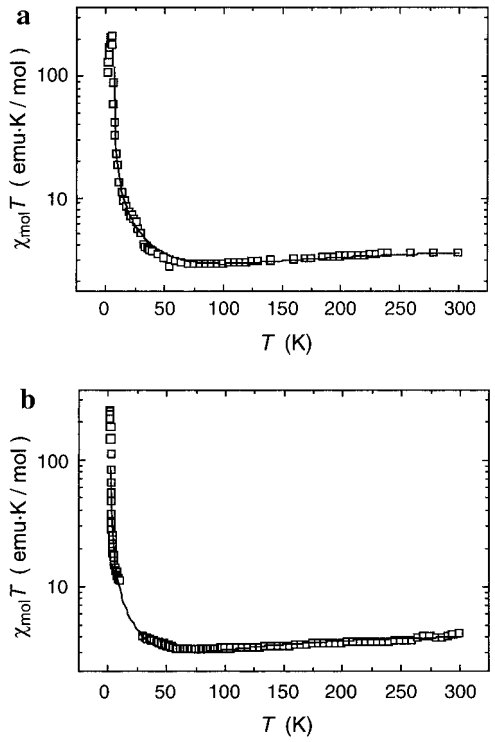

Figure 9. χ_{mol}·T vs T plots for the photolyzates of (a) complexes **a** and (b) **b**. The full lines correspond to the theoretical ones assuming (5/2 − 1) alternating chain models. The χ_{mol}·T values are presented in a logarithmic scale to stress the agreement near the minima at ca. 70 K.

and their temperature indepedence clearly indicated that both complexes [Mn(hfac)$_2$·**1**] are dilute d^5 Mn(II) paramagnets. After photolysis of the diazo moieties, the generated triplet carbene centers become capable of coupling with the d^5 Mn(II) ions coordinated at the pyridyl nitrogen atoms on either side in *antiferromagnetic* fashion as suggested by 1:2 model complexes of Mn(hfac)$_2$ with *N*-*tert*-butyl-*N*-(4-pyridyl)aminoxyl and phenyl(4-pyridyl)diazomethane reported previously.[4,6] Since this coupling is not necessarily strong compared with thermal fluctuation, temperature dependence shows a behavior characteristic of ferrimagnetic chains. At high temperature, $\chi_{mol}T$ values are lower than the 5.37 emu·K·mol^{-1} expected for an assembly of one S = 5/2 and one S = 1 spins in random orientation. As the temperature was decreased from 240 K, $\chi_{mol}T$ values for complexes **a** and **b** decreased gradually to shallow minima at ca. 80 K, showing the cancellation of a pair of one S = 5/2 and one S = 1 spins by antiferromagnetic coupling. As the temperature was lowered further, $\chi_{mol}T$ values started to increase rapidly in proportion to the increase in the correlation length of the ferrimagnetic chains. The $\chi_{mol}T$ values for complex **a** reached a maximum of 210 emu·K·mol^{-1} at 5 K and then decreased slightly until 1.9 K, while those for complex **b** did not reach a maximum until at least 1.9 K (246 emu·K·mol^{-1} at 1.9 K). The decrease of $\chi_{mol}T$ value observed below 5 K for complex **a** must be due to partial saturation of magnetization at the applied field of 20 Oe and/or antiferromagnetic interaction between the chains, although the chains looked well separated in the precursor diazo complexes [Mn(hfac)$_2$·**1**] from the X-ray crystal structure analysis. The observed history dependence of M values prevented us from investigating their magnetic behavior in detail in small applied fields at temperatures less than 5 K.

The observed temperature behavior for complexes **a** and **b** was similar and showed characteristic features of ferrimagnetic chains with an antiferromagnetic exchange parameter (J < 0). This antiferromagnetic interaction between the generated carbene and manganese ion is consistent with that revealed by using 1:2 manganese(II) complexes with 4-pyridyl(*N*-*tert*-butyl)-aminoxyls [Mn(hfac)$_2$(4NOPy)$_2$].[4] The maximum values (210 and 246 emu·K·mol^{-1}) for complexes **a** and **b** were used by application of eq 3[17] to estimate the correlation lengths $\xi(T)$ of 186 and 218 units of S = 3/2 made of antiferromagnetically coupled d^5 Mn and triplet carbene, respectively.

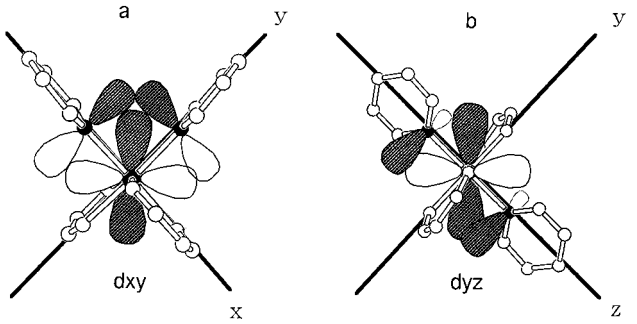

Figure 10. Illustrations of relative geometry between the manganese ions and coordinating pyridine rings for (a) complexes **a** and (b) **b** projected from the z and x axes, respectively.

$$\xi(T) = 2\chi(T)/S^2 - 1/S \qquad (3)$$

We note from comparison of the $\chi_{mol}T - T$ plots in Figures 4 and 5 that the $\chi_{mol}T$ values increase faster in complex **a** than complex **b** as we lower the temperature. This trend is conspicuous at temperatures below 10 K and suggests that the antiferromagnetic interaction between the generated carbene and manganese ion for complex **a** must be stronger than that for complex **b**. Actually, the data after irradiation for complexes **a** and **b** were analyzed theoretically on the basis of a ferrimagnetic chain model consisting of S = 5/2 classical and S = 2/2 quantum spins to give J/k_B = −34.8 and −24.4 K, respectively. The interchain interaction was estimated to be weakly ferromagnetic, although we could neither locate the origin of the ferromagnetic interaction nor detect a magnetic phase transition at temperatures higher than 1.9 K.

To elucidate the observed difference in the magnitude of J, the overlaps of 2p-orbital at the pyridyl nitrogen and 3d-orbitals of manganese ion on one hand and p_π-orbitals between the photogenerated carbene center and the pyridine ring on the other are considered to be important.[4,18] The relative geometry of the orbitals of the pyridine rings and the manganese ion revealed by X-ray molecular structures of complexes **a** and **b** having cis and trans coordination, respectively, is schematically illustrated in Figure 10. From bond lengths around the manganese ion, molecular z axes may be defined along the O(2)MnO(4) and N(1)MnN(1*) bonds for complex **a** and complex **b** in Figure 3, respectively. The manganese(II) ion has five unpaired electrons in d_{xy}, d_{xz}, d_{yz}, $d_{x^2-y^2}$, and d_{z^2} orbitals; the fist three of the five orbitals having π character might interact predominantly with the π-orbitals on the pyridyl nitrogens, while the remaining orbitals have no overlap with them. As shown in Figure 10, the π-orbitals of two pyridyl nitrogens for complex **a** are in the xy plane (parallel to the x or the y axis) and could overlap with

(17) $S(S + 1)/2$ was used in place of $\chi_c T$ in eq 5 in: Caneschi, A.; Gatteschi, D.; Sessoli, R. In *Magnetic Molecular Materials*; Gatteschi, D., Kahn, O., Miller, J. S., Palacio, F., Eds.; Kluwer: Dordrecht, 1991; p 223.

(18) Luneau, D.; Rey, P.; Laugier, J.; Fries, P.; Caneschi, A.; Gatteschi, D.; Sessoli, R. *J. Am. Chem. Soc.* **1991**, *113*, 1245−1251.

the d-orbitals, e.g., d_{xy} of the manganese ion. On the other hand, the planes of the two pyridine rings coordinated in the trans configuration for complex **b** are rotated by 41.03 ° around the *x* axis from the *yz* plane and the π-orbitals of the pyridine nitrogens are directed to the midpoint between d_{xz} and d_{yz} orbitals of the manganese(II) ion (Figure 10, part b). Therefore it is less overlapped with those of the manganese ion, making the interaction weaker. The dihedral angle of C(1)C(3)C(5)−C(1*)C(3*)C(5*) for complex **b** is smaller by ca. 10° than the corresponding value for **a**, suggesting the delocalization of the spin of the carbene center in complex **b** is greater than in complex **a**. However, this assumption could not explain the difference in *J* values of the complexes. It will be less effective for a magnetic interaction between the carbene and the manganese ion.

Such sharp changes in the $\chi_{mol}T$ values as observed in the corresponding copper complexes at around 230 K[5] were not observed in the $\chi_{mol}T - T$ plots for both Mn complexes. However, it was confirmed that the carbene centers still survived at around 200 K by decreasing the temperature from 200 K. In other words, the triplet carbenes are stable in the crystal lattice of the complex up to these temperatures.

Conclusion

Two isomeric bis(hexafluoroacetylacetonato)manganese complexes, **a** and **b**, with diazodi(4-pyridyl)methane (**1**) were prepared individually and were determined to have helical and zigzag chain structures in which the pyridyl nitrogen atoms of two different molecules of **1** are coordinated to the octahedral manganese ion in the cis and the trans configurations, respectively. The irradiation of the dilute paramagnetic manganese complexes converted the diazo groups to the triplet carbenes, thus effecting the *antiferromagneitc* coupling of the d^5 spins of the former with p and sp^2 spins of the latter by polarization of the π-electrons on the pyridine ring.

The correlation length extended over 186 and 218 manganese−carbene $S = 3/2$ units along the ferromagnetic chain at cryogenic temperature. These results provide the first example of the formation of extended *ferri*magnetic chains containing photochemically generated 2p spins: a prototype of the molecular photomagnetic recording device in which only the irradiated micro domain of the nonmagnetic or weakly magnetic materials becomes strongly magnetic. The extension of the correlation length is considerable in reference to the *ferromagnetic* chains formed by irradiation of the corresponding copper complex [Cu(hfac)$_2$·**1**] in which the correlation was estimated to be only ca. 23 units at 3 K. The observed longer correlation length in the manganese complexes of this work may be ascribed to the larger spin 5/2 of Mn(II) relative to 2/2 of Cu(II) and also to stronger antiferromagnetic interchain interaction in the latter.[5]

Acknowledgment. This work was supported by a Grant-in-Aid for Scientific Research (B)(2) (No. 09440242) and COE Research (No. 08CE2005) from the Ministry of Education, Science, Sports and Culture, Japan. One of the authors (N.K.) acknowledges the financial support from Asahi Glass Foundation.

Supporting Information Available: Field dependences of *M* for complexes **a** at 2 K (Figures S1) and **b** at 5 K (Figure S2); details of the crystallographic analysis of complex **a** and **b** of [Mn(hfac)$_2$·**1**] (51 pages, print/PDF). See any current masthead page for ordering information and Web access instructions.

JA981293N